

What causes the 24-day period observed in solar flares?

M. Temmer¹, J. Rybák², A. Veronig¹, and A. Hanslmeier¹

¹ Institute of Physics/IGAM, Universität Graz, Universitätsplatz 5, A-8010 Graz, Austria

² Astronomical Institute/SAS, SK-05960 Tatranská Lomnica, Slovak Republic

Preprint online version: January 13, 2005

Abstract. Previous studies report a ~ 24 -day (synodic) period in the occurrence rate of solar flares for each of the solar cycles studied, no. 19–22 (Bai 1987; Temmer et al. 2004). Here we study the 24-day period in the solar flare occurrence for solar cycles 21 and 22 by means of wavelet power spectra together with the solar flare locations in synoptic magnetic maps. We find that the 24-day peak revealed in the power spectra is just the result of a particular statistical clumping of data points, most probably caused by a characteristic longitudinal separation of about $+40^\circ$ to $+50^\circ$ of activity complexes in successive Carrington rotations. These complexes appear as parallel, diverging or converging branches in the synoptic magnetic maps and are particularly flare-productive.

Key words. Sun: flares – activity – magnetic fields

1. Introduction

A ~ 24 -day synodic period in the solar flare occurrence has been reported in various studies, but its origin is still far from being understood. Explanatory statements most often refer to the rotational behavior of the solar interior, i.e. deeper lying zones of activity connected to sunspots rotate faster than the solar photosphere (Bai 1987; Pap 1985; Pap et al. 1990). In the frame of the anchoring hypothesis (Balthasar et al. 1982), specifically new-born spots are connected to deeper and thus faster-rotating layers. However, from solar rotation studies based on tracing sunspots only a small fraction (of the order of 1%) of sunspots is reported with sidereal velocities as high as 16 deg/day corresponding to a ~ 24 -day synodic period (e.g. Godoli et al. 1998; Pulkkinen & Tuominen 1998; Suzuki 1998).

A 23.8-day¹ period in the solar flare occurrence was first reported by Bai (1987) for high-energetic hard X-ray events during cycle 21 for the years 1980–1985. It is worth noting that similar periods were also identified in other solar data sets. Pap (1985) and Pap et al. (1990) found a 23.5-day period in solar irradiance measurements for the time span 1980–1988 and in the occurrence rate of very young, hence active, sunspot groups. Temmer et al. (2003) found a prominent 23.8-day periodicity in the occurrence rate of major solar flares observed in H α during 1975–2001 which could not be established for sunspot relative numbers analyzed for the same time span. However, after

the removal of predominant periods, Zięba et al. (2001) identified a 23.8-day period in sunspot relative numbers during the rising phase of solar cycle 23. A slightly higher period of 24.4 days was found by Henney & Harvey (2002) in magnetic flux time series for the time span 1977–2001.

Recently, Temmer et al. (2004) performed a systematic study regarding a possible ~ 24 -day synodic period in the occurrence rate of solar flares for the time span 1955–1997. It was found that the 24-day period in solar flare rates is not an isolated phenomenon but occurred in all four solar cycles studied (no. 19–22), predominantly during narrow time ranges around the cycle maxima. For flares of H α importance classes ≥ 1 , the appearance of the 24-day period was more prominent but it could also be seen in subflares. In 3 out of 5 studied cases where a 24-day period was seen in major flare occurrence, a corresponding period was also found in the occurrence rate of magnetically complex active regions (including classification γ and/or δ), whereas it could not be established in magnetically non-complex (α , β) sunspot groups. These findings are suggestive of a close connection of the 24-day period seen in flare occurrence with the magnetic field evolution of complex active regions, which produce most large flares (e.g. Sammis et al. 2000).

In the present paper we aim to clarify the type of relation of the 24-day flare period to the magnetic field evolution, and therefore combine the statistical results from wavelet power spectra with active region magnetic data. Specifically, we analyze synoptic magnetic maps from the National Solar Observatory at Kitt Peak together with the occurrence rate of major H α flare events for times in which

Send offprint requests to: M. Temmer

Correspondence to: mat@igam.uni-graz.at

¹ All periods stated in this paper are synodic.

Table 1. Time spans for which the wavelet power spectra were calculated together with the solar cycle number and hemisphere (N – North, S – South).

Time span	Cycle no.	Hemisphere
1981.56–1983.75	21	N
1979.62–1981.81	21	S
1986.71–1988.69	22	N
1988.43–1990.62	22	S
1990.22–1992.41	22	S

a peak at ~ 24 days was revealed in the wavelet power spectra. As we will demonstrate in this study, the 24-day period manifested in the power spectra is a statistical result of the interplay between a characteristic longitudinal separation of $+40^\circ$ to $+50^\circ$ of active region complexes and the solar rotation period. Thus, we are not dealing here with a period properly, and will use the term "quasi-period" instead of "period" in the following.

2. Data

We analyze time intervals in which a 24-day quasi-period in the occurrence rate of major solar flares is reported by Temmer et al. (2004) for solar cycles 21 and 22. These are within the years 1982–1983 for the northern, and 1980–1981, 1989–1990 and 1991–1992 for the southern solar hemisphere. We also analyze the time span 1987–1989 for which we found a 24-day quasi-period for the northern hemisphere when considering only times of minimum solar activity (whereas in the study of Temmer et al. 2004 wavelet power spectra for an entire solar cycle were investigated). The exact time spans used for the analysis are listed in Table 1. Note that in order to reduce edge (cone of influence) effects, for the calculation of the wavelet power spectra somewhat larger (about ± 0.5 years) time intervals than reported in Temmer et al. (2004) were used for estimating the 24-day quasi-period.

Daily numbers of H α flare events for importance classes ≥ 1 ('major' flares) are derived separately for the northern and southern hemisphere, using the flare compilation from the Solar Geophysical Data. The magnetic synoptic maps employed are from the National Solar Observatory at Kitt Peak (NSO/KP). Each synoptic map is made from daily full-disk line-of-sight magnetograms of the Sun for a full Carrington Rotation (CR), i.e. 27.2753 days, and approximates the magnetic flux density in the photosphere as a function of heliographic longitude and latitude under the assumption that the magnetic fields are vertical (cf. Harvey et al. 1980; Gaizauskas et al. 1983; Worden & Harvey 2000, and references therein). Since NSO/KP synoptic maps are not available before 1973, only solar cycles 21 and 22 are studied.

3. Methods and Analysis

Wavelet power spectra are an appropriate tool for investigating time series that contain non-stationary power at

many different frequencies (Daubechies 1990). In particular, they can be used to determine predominant periods in a time series together with their times of appearance.

We use the Morlet wavelet (Grossman & Morlet 1984) as analyzing wavelet function $\psi(\tau)$, where τ is a non-dimensional time parameter. The continuous wavelet transform can be written as

$$W_n(s) = \sum_{k=0}^{N-1} \hat{x}_k \hat{\psi}^*(s\omega_k) e^{i\omega_k n \delta t}, \quad (1)$$

with δt the equal spacing in time, N the number of data points in the time series $\{x_n\}$, \hat{x}_k the discrete Fourier transform of x_n and $\hat{\psi}^*(s\omega_k)$ the scaled and translated version of $\psi(\tau)$ (* indicates the complex conjugate). The angular frequency ω_k is defined as

$$\omega_k = \begin{cases} \frac{2\pi k}{N\delta t} & : k \leq \frac{N}{2} \\ -\frac{2\pi k}{N\delta t} & : k > \frac{N}{2}. \end{cases} \quad (2)$$

With the actual choice for the value of ω , one can specify either a high resolution in time or a high resolution in frequency. For our purpose we have chosen the values $\omega = 48$ to obtain a high frequency resolution and $\omega = 6$ to obtain a high temporal resolution. All wavelet power spectra (WPS) presented in this paper were calculated for the period range 20–30 days. As significance tests, confidence levels at 90%, 95%, and 99% are calculated using a red noise background spectrum based on the assumption that daily flare data are correlated (Oliver & Ballester 1995). Regions where edge effects become important because we are dealing with finite-length time series, such as the beginning and the end of the wavelet spectrum, are labeled as cone of influence (COI). The computation of all these parameters is performed in the way described by Torrence & Compo (1998).

The data analysis is performed as follows. For each time period listed in Table 1 we calculated wavelet power spectra from daily numbers of H α flares ≥ 1 with a) high angular frequency ($\omega = 48$) in order to obtain a high frequency resolution, and b) low angular frequency ($\omega = 6$) in order to obtain a high temporal resolution. The derived WPS are shown in the top panels of Figs. 1–5 (left: $\omega = 48$, right: $\omega = 6$). For a clearer representation, we did not plot the total time range for which the WPS was calculated (i.e. the times listed in Table 1) but only narrow ranges in which the 24-day quasi-period distinctly shows up. After locating the appearance of the ~ 24 -day quasi-period precisely in time (using the WPS calculated with $\omega = 6$), the synoptic magnetic maps of the relevant time span were selected. The heliographic coordinates and times of the associated flares were mapped to the corresponding Carrington rotation number and Carrington longitude (L), and superimposed on the synoptic magnetic maps (bottom panels of Figures 1–5). Since the determination of the heliographic longitude of a flare close to the limb is very sensitive to small errors, only flares with a distance $\leq 60^\circ$ from the central meridian were taken into account.

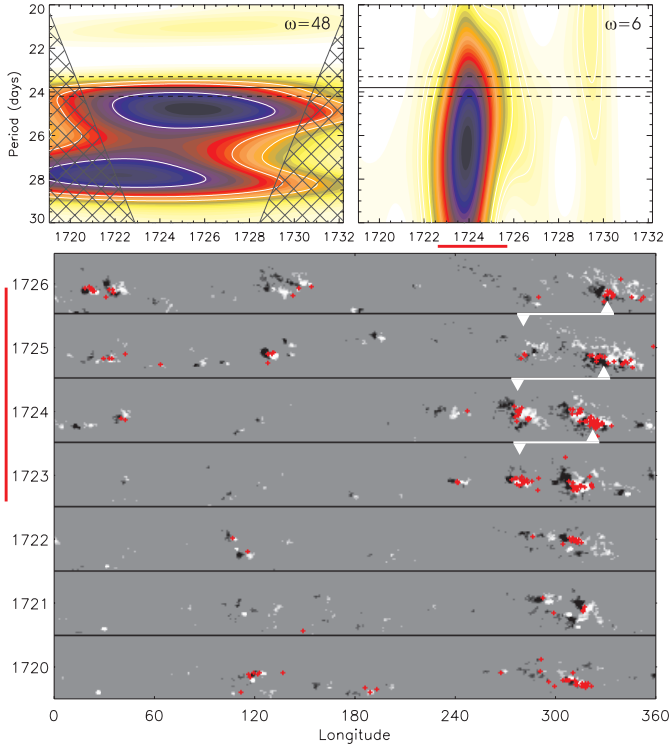


Fig. 1. Top: WPS derived from daily rates of major flares for the northern hemisphere during CR 1720–1732 (cycle 21: 1982 March–1983 February) with angular frequency values $\omega = 48$ (left) and $\omega = 6$ (right). Color coding from yellow to black represents the square root of the power on a linear scale. White contour lines from thin to thick denote confidence levels at 90%, 95% and 99%. Cross-hatched lines mark the COI. The red bar indicates the time range where strong power occurs in the WPS. Horizontal solid and dashed lines are drawn for periods of 23.8 ± 0.5 days, respectively. Bottom: Strips of synoptic magnetic maps for the belt $N0^\circ$ – $N40^\circ$ for CR 1720–1726 (1982 March–1982 September). The line-of-sight component of the magnetic field is represented as white/black for positive/negative polarity. Red crosses indicate the positions of flare events ≥ 1 . White arrows mark the separation between two flare-producing active regions in successive Carrington rotations which correspond to a quasi-period of ~ 24 days.

4. Results

Figures 1–5 show the WPS calculated from time series of daily numbers of $H\alpha$ flares with importance classes ≥ 1 (cf. Table 1 for the exact time ranges analyzed) with high frequency (top left) and high time (top right) resolution together with the corresponding synoptic magnetic maps including the individual flare positions (bottom). Here we draw attention to high amplitudes in the WPS within a confidence level of at least 95% observed for the period range 23.8 ± 0.5 days (a 23.8-day quasi-period is reported by Bai 1987; Zięba et al. 2001; Temmer et al. 2003, 2004). Note that we do not concentrate on periods related to the solar differential rotation (which are also present in the WPS shown in Figs. 1–5). Mean synodic periods reported for the differential rotation of the Sun are within ~ 26.5

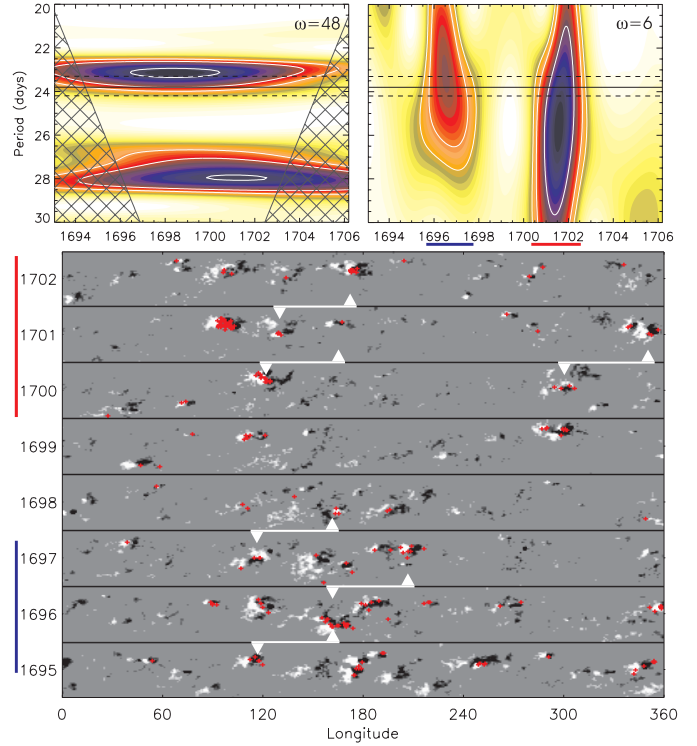


Fig. 2. Same as Fig. 1 but for the southern hemisphere during CR 1693–1706 (cycle 21: 1980 March–1981 March). Red and blue bars indicate time ranges where strong and faint power occurs in the WPS, respectively. Strips of synoptic magnetic maps are for the belt $S0^\circ$ – $S40^\circ$ for CR 1695–1702 (1980 May–1980 December).

days near the solar equator and ~ 29.5 days around 40° latitude (e.g., Howard 1984; Balthasar et al. 1986). For the interpretation of synoptic maps it is important to note that active regions forming a vertical band in successive CRs have rotational periods close to the CR period of ~ 27.3 days, whereas bands revealing a slope to the left (i.e. toward smaller Carrington longitudes) have periods longer than the CR period and bands inclined to the right (i.e. toward higher Carrington longitudes) have shorter periods than the CR rate.

The high-frequency resolution WPS in Fig. 1 (top left panel) shows a broad range within the spectrum where local peaks of from ~ 23.5 to ~ 28.7 days are revealed above the significance level of 95%. At a significance level of 99%, two dominant peaks centered at ~ 24.7 and ~ 28.0 days can be distinguished. As can be seen from the high-time-resolution WPS calculated for the same time span (top right panel), these peaks appear during CR 1723 to CR 1726 (on a 99% significance level). The corresponding synoptic maps (bottom panel) reveal that the majority of flares occurs in a diverging active region with the intersection point centered at Carrington longitude $L \sim 310^\circ$ at CR 1720. Using the flare locations as tracers, the longitudinal separation of the two branches of the diverging active region is $\sim 45^\circ$ between the successive Carrington rotations 1723/1724, $\sim 52^\circ$ between CR 1724/1725, and

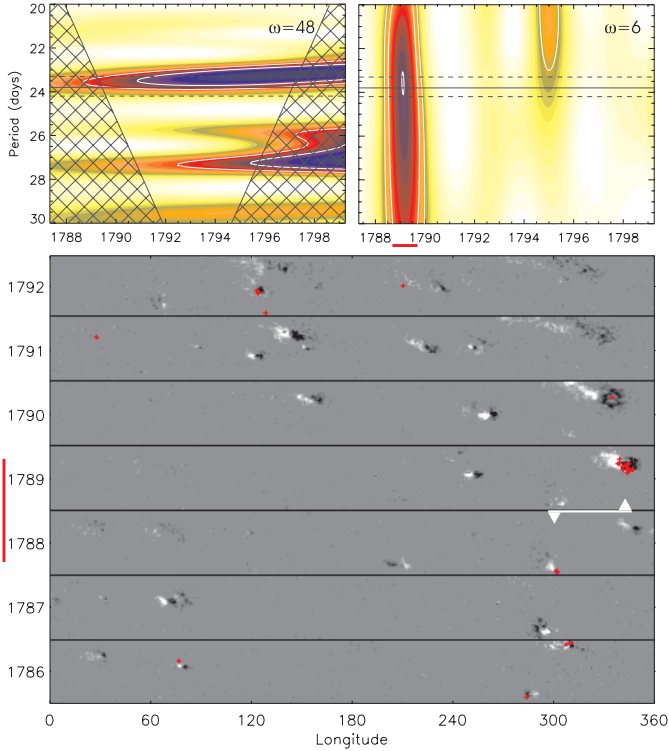


Fig. 3. Same as Fig. 1 but for the northern hemisphere during CR 1786–1799 (cycle 22: 1987 February–1988 February). Strips of synoptic magnetic maps are for the belt $N0^{\circ}$ – $N40^{\circ}$ for CR 1786–1792 (1987 February–1987 August).

ends up with $\sim 51^{\circ}$ between CR 1725/1726 (indicated by white arrows in Fig. 1).

It is important to note that longitudinal differences between successive CRs in the range $+40^{\circ}$ to $+50^{\circ}$ correspond to a difference of -3.0 to -3.8 days with respect to the Carrington rotation rate of ~ 27.3 days, i.e. quasi-periods in the range 23.5 to 24.3 days. This can be interpreted in terms of a *rotational* period only in cases where such a longitudinal shift between consecutive CRs is observed for the *same* feature. In the synoptic maps in Fig. 1, however, this shift is observed between the two branches of a flare-productive diverging active region complex, and thus has nothing to do with rotation at all. However, it seems to be the cause of the ~ 24 -day quasi-period revealed in the WPS during the same time. As will be shown in the following, a similar outcome is obtained for the other samples.

The wavelet power spectra in Fig. 2 reveal a quasi-period of about 23.3 days during CR 1696–1698 (faint signal) and CR 1700–1702 (strong signal), respectively. Additionally, for CR 1700–1702 enhanced power in the wavelet spectra is observed at ~ 28 days. During these two time spans, in the synoptic maps patterns of parallel bands of active regions responsible for a significant fraction of major flares are observed. These bands are separated in longitude by about 45° – 50° , which corresponds to a quasi-

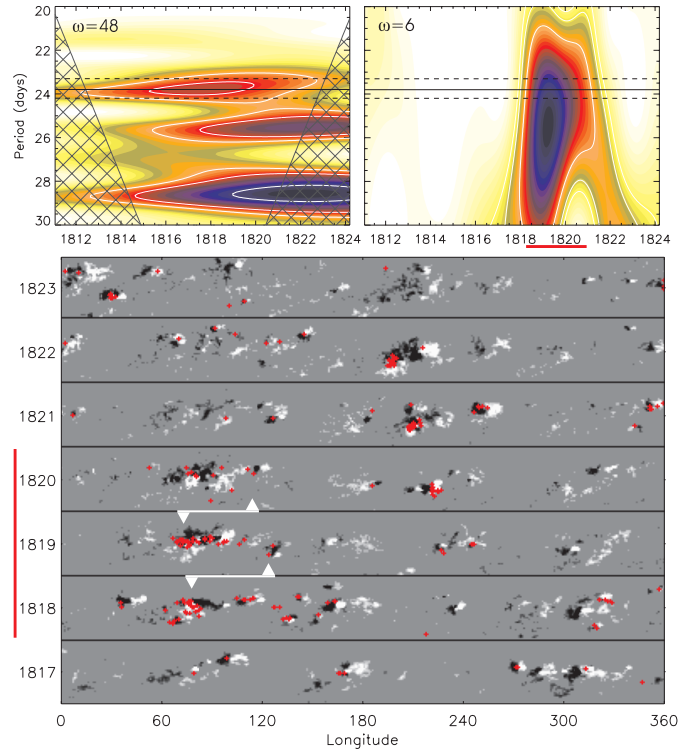


Fig. 4. Same as Fig. 1 but for the southern hemisphere during CR 1812–1825 (cycle 22: 1989 February–1990 January). Strips of synoptic magnetic maps are for the belt $S0^{\circ}$ – $S40^{\circ}$ for CR 1817–1823 (1989 June–1989 December).

period in the range of 23.5–23.9 days, similar to what is actually observed in the WPS.

In Fig. 3 the occurrence of major flares during the initial phase of solar cycle 22 is studied. This sample differs from the others as it covers a time of minimum solar activity. In the WPS, a quasi-period of about 23.5 days is revealed very sharply in time during CR 1788–1789. Only few active regions are present on the Sun, and during the considered interval only two active regions were observed that produced major flares; these regions were separated in longitude from CR 1788 to CR 1789 by about 43° which corresponds to a quasi-period of ~ 24.0 days.

From the WPS in Fig. 4 a significant (95% confidence level) power signal is obtained with a quasi-period of 23.8 days during CR 1818–1820. During this time, the synoptic maps reveal two converging branches of active regions which are responsible for the majority of solar flares. The two branches are separated by $\sim 45^{\circ}$ in longitude in successive CRs corresponding to a quasi-period of 23.9 days, again close to what is observed in the WPS.

In Fig. 5 a clear quasi-period in the range of about 23.8 days is revealed from the WPS within CR 1838–1840. During this time span the synoptic magnetic maps show two nearly parallel bands of high flare activity shifted by $\sim 46^{\circ}$, 35° , and 47° within the successive rotations 1838/1839, 1839/1840, and 1840/1841, respectively. This would cause quasi-periods of ~ 23.8 , 24.7, and 23.7 days.

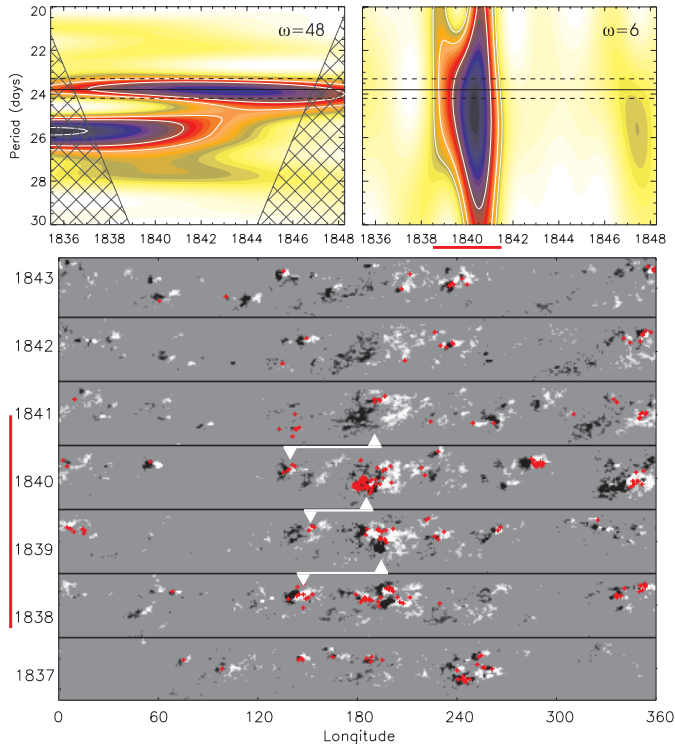


Fig. 5. Same as Fig. 1 but for the southern hemisphere during CR 1836–1848 (cycle 22: 1990 November–1991 October). Strips of synoptic magnetic maps are for the belt S0°–S40° for CR 1837–1843 (1990 December–1991 June).

5. Discussion

The combined analysis of wavelet power spectra and synoptic magnetic maps provides us with the possibility to locate the appearance of the 24-day quasi-period in solar flare occurrence both statistically and individually. The flare location in the synoptic maps suggests that peaks in power spectra of 24 days which were found in the occurrence of flares observed in hard X-rays (Bai 1987) and $H\alpha$ (Temmer et al. 2003, 2004), in magnetic flux time series (Henney & Harvey 2002), in active region time series (Pap 1985; Pap et al. 1990; Zięba et al. 2001) and in the occurrence rates of magnetically complex active regions (Temmer et al. 2004) can be explained by the spatial distribution of complex, flare-productive active regions. In general, active regions are not randomly distributed but are clustered within so-called complexes (‘nests’) of activity (Bumba & Howard 1965). These clusters typically evolve within one month and are sustained by the fresh emergence of magnetic flux for about 3–6 months (Gaizauskas et al. 1983).

Flare-producing nests separated by about $+40^\circ$ to $+50^\circ$ in longitude within successive rotations would cause periods shorter than the Carrington rotation by -3.0 to -3.8 days, i.e. the corresponding quasi-periods are in the range 23.5 to 24.2 days. Our analysis showed that when flare-productive activity nests with such characteristics are observed in the synoptic maps, these quasi-periods are

indeed observed simultaneously in the wavelet power spectra. (Actually, our approach was the other way round, as we first checked the WPS for the occurrence of a ~ 24 -day quasi-period and then inspected the synoptic maps during the times of appearance of the 24-day quasi-period.) If this interpretation is correct, then the WPS should also reveal a peak in the range of ~ 3 – 4 days which reflects directly the characteristic separation in longitude. We checked this by calculating WPS for the same time spans as listed in Table 1 but ranging from 2 to 30 days. In ‘simple’ situations (i.e. clearly separated activity branches and low flare activity from other active regions), indeed peaks in the range 3–4 days are revealed in the WPS above a confidence level of 95%.

Clearly separated nests of activity are evident in Figs. 1, 3, and 5. The synoptic maps of Figs. 2 and 4 show more loose-activity complexes of ambiguous separation and thus are less convincing samples. On the other hand, it is apparent, e.g., from the synoptic maps in Fig. 2, that the absence of such spatially divided activity nests (cf., CR 1698–1700) coincides with the absence of a 24-day quasi-period in the WPS.

Gaizauskas et al. (1983) described exemplary shapes of multiple complexes of activity, namely ‘great complexes’ consisting of two parallel main branches separated by about 40° in longitude as well as ‘diverging and merging complexes’ with two branches that diverge and converge, respectively, within successive rotations. These patterns are attributed to a regularity in the spacing between the complexes with distances that depend on the characteristic sizes of the regions (Gaizauskas et al. 1983). Thus, these spatial separations are supposed to be a non-random phenomenon which might be related to typical size scales of giant (convective) cells which have typical longitudinal extensions of 40° – 50° and are assumed to play an important role in structuring the Sun’s large-scale magnetic field (Bumba & Howard 1965; Beck et al. 1998). It is also worth noting that Pojoga & Cudnik (2002) found that ~ 70 – 75% of all flares occur within activity nests, and that parallel, converging and diverging activity nests exhibit enhanced flare productivity.

Following the reports from the Mount Wilson Observatory, most active regions within the studied synoptic maps are classified as magnetically complex, i.e. include γ and/or δ groups. There are no spatially divided patterns causing a quasi-period of 24 days that consist solely of magnetically non-complex groups.

6. Conclusion

The 24-day quasi-period was statistically found in the occurrence of major solar flares in each of solar cycles 19 to 22 (Bai 1987; Temmer et al. 2004). In this paper, we have compared the statistical appearance of the 24-day quasi-period in wavelet power spectra (with high temporal resolution) with the occurrence of individual major flare events in synoptic magnetic maps. From this analysis we conclude that the 24-day peak revealed in power spectra is

just the result of a particular statistical clumping of data points. The 24-day quasi-period in fact results from the interplay between the solar rotation period and a typical separation in longitude by $+40^\circ$ to $+50^\circ$ of large parallel, diverging, or converging activity nests in successive CRs. Such regions are known to be particularly flare-productive (Pojoga & Cudnik 2002). It is worth noting that these longitudinal separations are of the same size as those reported for giant convective cells (Beck et al. 1998).

Acknowledgements. M.T., A.V., and A.H. gratefully acknowledge the Austrian *Fonds zur Förderung der wissenschaftlichen Forschung* (FWF grant P15344) and J.R. the Slovak grant agency VEGA (2/3015/23) for supporting this project. J.R. is member of the European Solar Magnetism Network (ESMN) supported by the EC (EC/RTN contract HPRN-CT-2002-00313). M.T., A.H., and J.R. thank the Austrian and Slovak Academies of Sciences for financing the exchange of scientists. We also want to thank the referee J. Pelt for his constructive comments. NSO/Kitt Peak data used here are produced cooperatively by NSF/NOAO, NASA/GSFC, and NOAA/SEL. Wavelet software was provided by C. Torrence and G. Compo (<http://paos.colorado.edu/research/wavelets/>).

References

- Bai, T. 1987, *ApJ*, 314, 795
- Balthasar, H., Schüssler, M., & Wöhl, H. 1982, *Sol. Phys.*, 76, 21
- Balthasar, H., Vázquez, M., & Wöhl, H. 1986, *A&A*, 155, 87
- Beck, J., Duvall, T., & Scherrer, P. 1998, *Nature*, 394, 653
- Bumba, V. & Howard, R. 1965, *ApJ*, 141, 1502
- Daubechies, I. 1990, *IEEE Transactions on Information Theory*, 36, 961
- Gaizauskas, V., Harvey, K. L., Harvey, J. W., & Zwaan, C. 1983, *ApJ*, 265, 1056
- Godoli, G., Mazzucconi, F., & Piergianni, I. 1998, *Sol. Phys.*, 181, 295
- Grossman, A. & Morlet, J. 1984, *SIAM J. Math.*, 15, 723
- Harvey, J., Gillespie, B., Miedaner, P., & Slaughter, C. 1980, *NASA STI/Recon Technical Report N*, 81, 21003
- Henney, C. J. & Harvey, J. W. 2002, *Sol. Phys.*, 207, 199
- Howard, R. 1984, *ARA&A*, 22, 131
- Oliver, R. & Ballester, J. L. 1995, *Sol. Phys.*, 156, 145
- Pap, J. 1985, *Sol. Phys.*, 97, 21
- Pap, J., Bouwer, S. D., & Tobiska, W. K. 1990, *Sol. Phys.*, 129, 165
- Pojoga, S. & Cudnik, B. 2002, *Sol. Phys.*, 208, 17
- Pulkkinen, P. & Tuominen, I. 1998, *A&A*, 332, 748
- Sammis, I., Tang, F., & Zirin, H. 2000, *ApJ*, 540, 583
- Suzuki, M. 1998, *Sol. Phys.*, 178, 259
- Temmer, M., Veronig, A., Rybák, J., & Hanslmeier, A. 2003, *Hvar Observatory Bulletin*, 27, 59
- Temmer, M., Veronig, A., Rybák, R., Brajša, R., & Hanslmeier, A. 2004, *Sol. Phys.*, 221, 325
- Torrence, C. & Compo, G. P. 1998, *Bulletin of the American Meteorological Society*, vol. 79, Issue 1, 79, 61
- Worden, J. & Harvey, J. 2000, *Sol. Phys.*, 195, 247
- Zięba, S., Masłowski, J., Michalec, A., & Kułak, A. 2001, *A&A*, 377, 297